

Ultra-fast catalytic detoxification of organophosphates by nano-zeolitic imidazolate frameworks



Arash Ebrahimi^a, Ehsan Nassireslami^{a,*}, Ramin Zibaseresht^{b,c}, Maedeh Mohammadsalehi^d

^a Department of Pharmacology & Toxicology, Faculty of Medicine, Aja University of Medical Sciences, Tehran, Iran

^b Biomaterials and Medicinal Chemistry Research Center, Aja University of Medical Sciences, Tehran, Iran

^c Department of Chemistry and Physics, Faculty of Sciences, Maritime University of Imam Khomeini, Nowshahr, Iran

^d Department of Pharmaceutical Chemistry, Pharmaceutical Sciences Branch, Islamic Azad University, Tehran, Iran

ARTICLE INFO

Keywords:

Zeolitic imidazolate frameworks
Catalytic detoxification
Hydrolysis
Organophosphates simulant
Diazinon

ABSTRACT

Detrimental and injurious impacts of Organophosphates that have had on environment, humans, organisms and the other animals or plants have not been surreptitious to anyone worldwide. Nevertheless, up to now, among many efforts that have been devoted to detoxification of Organophosphates (OPs), catalytic detoxification has been the most applicable, cost-effective, efficacious and safest way to break down these dangerous materials. Herein, the utilization of zeolitic imidazolate frameworks (ZIFs), for the first time, has been reported to deactivate Diazinon as an organophosphate agent demonstrated at room temperature. In the following research, the catalysts were analyzed by PXRD, FT-IR, FE-SEM, BET, CO₂ adsorption/desorption and TG. The decontamination processes were followed by ³¹P NMR, HPLC, and UV-vis to evaluate catalytic efficiency. Interestingly, supreme reusability, durability and potentially stunning catalytic activity represent them as alternate materials for their amazing elimination of OPs compared to the other MOFs.

1. Introduction

Demanding for detoxification of Organophosphates (OPs) such as Diazinon and Malathion due to their high toxicity and their environmentally deleterious effects on natural surroundings and individuals have been growing of concerns in recent years [1–3]. Among them, the case Organophosphorus pesticides (OPs) as highly venomous compounds have broadly used for agriculture [4,5]. Owing to their dangerous effects on organisms may cause paralysis and organ inabilities [6,7]. Moreover, Diazinon is also admitted as paronymous organophosphate pesticide with the virtue of relatively high toxicity should be examined to compare the analogous efficacy of the catalysts [1]. Lately, much more concerns in expanding the methodologies for catalytic detoxification of phosphate ester bond as a challenging issue have been ongoing to investigate the removal of such OPs [1,8]. Even though, it is mandatory to try developing the strategies that they have been helpful to degrade the P–O bonds employing the hydrolytic cleavage catalytically as the most advantageous method so far.

As regards, recently, various efforts have been utilized to overcome these barriers which have been carried out by exploiting the hydrolysis manner. Most of them have been manipulated by Farha et al. [9–13] are illustrative of its significant importance insisting on its simplicity, the

most extensively applicable and the most convenient procedure in terms of practicability, efficiency and turnover as well as productivity compared to others.

Of highly efficient and superior materials showing to degrade such pesticides [12,14–21], metal-organic frameworks (MOFs), a novel subdivision of crystalline porous materials, formed through bridging metal ions or clusters to the ligands in diverse topologies [22–27]. Owing to their tunable porosity, versatile flexible structural frameworks, remarkably high surface areas and post-synthesis of modified architectures with functional groups proven to be promising as an attractive material in diverse applications namely CO₂ capture [28], gas adsorption/storage [29], separation [30,31], photoluminescence [32], catalysis [33,34], chemical sensing [35,36] and drug delivery [37]. As subfamily of MOFs, zeolitic imidazolate frameworks (ZIFs), are hybrid material possessing simultaneously characteristics of both zeolite and MOFs such as chemical and thermal stability, crystallinity, chemical versatility, hydrophobic surfaces [38,39] which are basically made up of tetrahedral coordinated metal ions (Zn²⁺, Co²⁺, Cu²⁺) and imidazolate ligands in a 3D neutral open frameworks [40]. Existence of both acidic and basic functionality on ZIFs at the same time which induces by metal nodes and imidazolate groups, respectively, execute the heterogeneous catalytic activity, properly [41,42].

* Corresponding author.

E-mail address: nassireslami@gmail.com (E. Nassireslami).

Highly active phosphotriesterase (PTE) enzyme, has been recognized to be an effective agent in the hydrolysis of the P–O bond [43,44]. Considering the similarity of catalytic and structural aspects between PTE and ZIFs, in the case of PTE, a pair of Zn (II) ions compose the active site of PTE linked by OH ligand and enclosed by 2–3 nitrogen-based donor ligands (histidine imidazole). On the other hand, the Zn(II) and imidazolate sites in ZIFs can function collaboratively to accomplish the cleavage of P–O bonds; in both, Zn(II) center attaches and gives rise to activate the P–O bond whereas others trigger to transfer an OH[−] to inspire the breakage of an –OR moiety [9,10,45].

To date, most of catalytic detoxification and capture of OPs have been operated prosperously by MOF materials especially by water-stable mesoporous Zr-based MOFs and methyl paraoxon simulant and less performed by the other MOFs like CuBTC-MOF and/or by the other pesticides at room temperature in aqueous solution [12,14–21]. Avoiding long story but to name some recently outstanding of them in order to make it clear, many of previously demonstration of such works have been provided. Specifically, degradation of OPs performed by Ryu et al. [46] which were utilized by MOF-808, UiO-66 and UiO-66-NH₂ series in neat and aqueous solutions at room temperature showed half-life time of optimized MOF-808 equaled to 0.7 min. Navarro research group illustrated the synergistic properties of Zirconium-based MOFs and some certain functional group employing nucleophilic basic functionality linked to the organic linker and basic lithium alkoxides incorporated within their framework to boost their catalytic proficiency; with UiO-66-0.25NH₂@LiO^tBu presenting the most great rate ($t_{1/2} = 0.4$ min) displayed a favorable harmony between framework approachability and nucleophilicity of the materials [47]. The other example of similar work has been operated by Koning et al. [48] using UiO-66-NH₂, NU-1000, MOF-808, and PCN-777 in buffer solutions were assessed to decompose some chemically dangerous OPs. The observations there represented to reveal the main characteristics and mechanism that control these detoxification reactions resulted in tremendously swift hydrolysis rates which terminated to complete breakdown of pesticide during the reaction time only up to 5.5 min. More obviously, the two prominent researches virtually resembled to our work done by Farha et al. exceptionally encouraged us to execute similar work. In both of their work, they studied the catalytic detoxification of methyl paraoxon simulant agents where engaging NU-901 [49] and MOF-808 (6-connected) [10] as detoxifier to attack and finally to assert their highly active catalytic performances. In the former case (NU-901), also showed the comparison between the efficiency of less-volatile branched polymers and dendrimers to the volatile *N*-ethylmorpholine solution as buffer additives to accelerate the reaction. The examination displayed the decrease in reaction half-life time up to < 2 min declaring that amino-functionalized branched polymers and dendrimers would assist as an efficacious alternative bases for hydrolysis which could be nearly the same as *N*-ethylmorpholine. On the other hand, for the latter case (MOF-808 (6-connected)), the half-life time and the situation of the reaction were more relatively identical to our study which motivated us more to evaluate the application of a series of ZIFs catalyst in OPs decontamination. In this case, the optimized MOF-808 (6-connected) would successfully prosper to degrade simulant with less than 6 min of reaction time and half-life of < 0.5 min. Besides, the turnover frequency (TOF) value was more than 1.4 s^{−1} which was meaningfully much higher compared to those MOFs investigated in this survey. As shown below, for more clarified comparison the described data were gathered in Table 1.

With keeping these viewpoints in mind, we have postulated that ZIF materials also could prove their potential ability as great alternatives in detoxification of Organophosphates. Regarding to the best of our knowledge, heretofore, no catalytic reaction has been applied using ZIFs for decontamination of Diazinon and the other OPs.

Moreover, regarding the high toxicity of organophosphates and possibility of their being high-risk in exploiting them, mainly in the vapor state, we tended to assess the catalytic activity of ZIFs employing

Table 1

Summary of mainly recent experiments data obtained in hydrolysis degradation by various MOFs toward diverse Organophosphates.

MOF	Amount of catalyst [mg]	$t_{1/2}$ [min]	TOF [s ^{−1}]	Ref
MOF-808	20	0.7	1.05	[46]
UiO-66-0.25NH ₂ @LiO ^t Bu	20	0.4	1.7	[47]
PCN-777	1–2	0.5	1.5	[48]
NU-901	3.3	< 2	0.14	[49]
MOF-808	1.1	< 0.5	> 1.4	[10]
ZIF-8	1	0.5	> 1.3	–
(Our work)				

Diazinon to illustrate their exceptionally resembling performance compared either with MOFs or with other pesticides. In fact, in follow-up contribution, what we are trying to do is to examine the catalytic activity of nanocrystals of ZIF-7 and ZIF-8 toward Diazinon as Organophosphate, which has been confirmed by ³¹P NMR, HPLC, and UV–vis spectra. Finally, all the consequences ascertain that these materials can be executed as ultra-highly efficacious materials comparable to those which have been already reported.

2. Experimental

2.1. Materials

All the chemicals including Benzimidazole (C₇H₆N₂, 98%), 2-Methylimidazole (C₄H₆N₂, 99%), Ammonia solution (NH₃, 25%, 7 M), Absolute ethanol (C₂H₅OH, 96%), Zinc nitrate tetrahydrate (Zn(NO₃)₂·4H₂O, 98.5%), Diazinon (C₁₂H₂₁N₂O₃PS, 96%), Acetonitrile anhydrous (99.8%, HPLC grade) and *N*-ethylmorpholine (C₆H₁₃NO, 97%) were provided from Merck and Sigma-Aldrich and executed as received without any excessive purification.

2.2. Fabrication of materials (ZIF-7 and ZIF-8)

All the fabrications were conducted based on our previous manner with some modifications [50]. Briefly, in the case of ZIF-7, 0.118 g BIM (Benzimidazole; 1 mmol) was dispersed in 10 mL ethanol. Then, 0.130 g Zn(NO₃)₂·4H₂O (0.5 mmol) was poured into the solution. The mixture and the other 10 mL vial encompassing 5 mL of ammonia were placed in tightly capped 250 mL Teflon-lined autoclave. After 5 min stirring, the solution was kept under the ammonia atmosphere at room temperature for 30 min. The precipitate was completely centrifuged and rinsed with absolute ethanol two times and dried in the air for 24 h (Sample 1 (S1)).

Concerning ZIF-8, 0.082 g 2-mIM (2-Methylimidazole; 1 mmol) was dissolved in 10 mL ethanol. Afterward, 0.130 g Zn(NO₃)₂·4H₂O (0.5 mmol) was added into the solution. The mixture was tightly capped in 250 mL Teflon-lined autoclave under 5 mL of ammonia atmosphere at room temperature for 10 min stirring. Then, the residue was gathered by centrifugation, two times washed with ethanol, dried and kept overnight in the air (Sample 2 (S2)).

2.3. Instrumentation

X-ray diffraction patterns of the as-fabricated materials were conducted on a Phillips X'Pert Pro X-ray diffractometer with Cu K α ($\lambda = 1.5418$ Å) radiation at a scan rate of 2 degrees per minute with a step size of 0.028. Fourier transform infrared (FT-IR) spectra were obtained on a Nicolet Magna 550 spectroscope with the KBr pellet technique in the range of 4000–400 cm^{−1}. Field-emission scanning electron microscopy (FE-SEM) images were gained by a Zeiss model SIGMA VP-500 (Germany). BET experiments were measured at liquid N₂

temperature (77 K) operating a volumetric adsorption analyzer (BELSORP Mini from Microtrac Bel Corp. Co). CO₂ ads-des examination was carried out at 273 K (Microtrac BELSORP-HP analyzer) which the samples were degassed in the high vacuum at 423 K for 3 h before the measurements. Thermal gravimetric analysis (TGA) was performed on a Netzsch STA 409 PC/PG thermal analyzer (Germany) in argon gas atmosphere from 27 up to 750 °C in a heating rate of 20 °C min⁻¹. Hydrolysis progress illustrated by NMR spectra were collected on The Bruker Avance III 400 MHz NMR spectrometer. HPLC evaluations were recorded by an instrument (Agilent 1200 series) equipped with a UV-vis detector fixed at λ_{\max} = 254 nm. UV-vis spectra were gathered in the range of 200–800 nm by Shimadzu 2100 spectrophotometer at room temperature.

2.4. Catalytic activity examinations

2.4.1. ³¹P NMR studies

³¹P NMR measurements were recorded at room temperature. The reactions were operated based on Farha et al. methods with some rectification [10]. In brief, 1 mg of catalysts (S1 (3.31 μmol) and S2 (4.36 μmol)) were separately poured into 1 mL H₂O in a 10 mL vial. Then, adding solution of *N*-ethylmorpholine 0.45 M (1 mL solution; 0.05 mL *N*-ethylmorpholine, 0.9 mL DI water/0.1 mL D₂O) and stirring for 5 min to disperse homogeneously. Next, Diazinon (5 μL; 18 μmol) was added to the mixture solution. Then, after certain interval times (1–6 min for S1 and 1–4 min for S2), the reaction mixtures were filtered by a syringe filter (0.22 μm pores). Afterwards, the mixtures were immediately transferred to an NMR tube each separately and the spectra were collected instantaneously shortly after the start of the reaction. The first spectrum was measured at 1 min after adding of Diazinon and the remaining solutions were recorded at 4, 6, 20 min and 5 days for S2, S1, S2 post-filtration and Diazinon (in the absence of catalysts) by in situ ³¹P NMR, respectively.

2.4.2. HPLC measurements

Similar procedures were applied for HPLC and UV-vis experiments. Instead, after filtrations, 30 μL of residue was injected into the HPLC apparatus (mobile phase: water/acetonitrile (65/35); stable phase: reverse phase C₁₈, column temperature 25 °C at a rate of 1 mL/min) equipped with a UV-vis detector fixed at λ_{\max} = 254 nm especially for detection of Diazinon and 2-isopropyl-6-methyl-4-pyrimidinol (IMP) at ambient temperature. Besides, excess of 10 min were required to re-instate the primary condition to gather the next sample spectra.

2.4.3. UV-vis spectra tests

Furthermore, UV-vis investigations were run and evaluated under similar environments at room temperature. Progress of the reactions were analyzed by taking a 300 μL liquid from the mixtures and diluted by adding an aqueous solution of *N*-ethylmorpholine (5 mL, 0.45 M) before injection to UV/Vis instrument. Reactions' profiles were obtained by absorbance at several specified time with the increment of each 25 s up to 4 min in the range of 200–800 nm.

2.4.4. Heterogeneous trait and recycling inspections

Additionally, the authentication of the heterogeneity property of catalyst (S2) was corroborated by filtration via 0.22 μm syringe after stopping the reaction at minute 1 which was calculated for 20 min.

To examine the reusability of ZIF (S2), Diazinon hydrolysis processes were run in five times one after another. After the termination of each cycle, the catalyst was gathered by centrifugation from container vial and then the solvent was removed. To rinse any product such as unwanted and un-reacted materials from the outermost surface and structure of ZIF, the process was operated for 3 times where after adding 2 mL of 0.15 M *N*-ethylmorpholine to the vial containing the catalyst, the solution was then stirred for 20 min. Next, after stirring, the solvent was eliminated. Finally, the solid was washed with ethanol

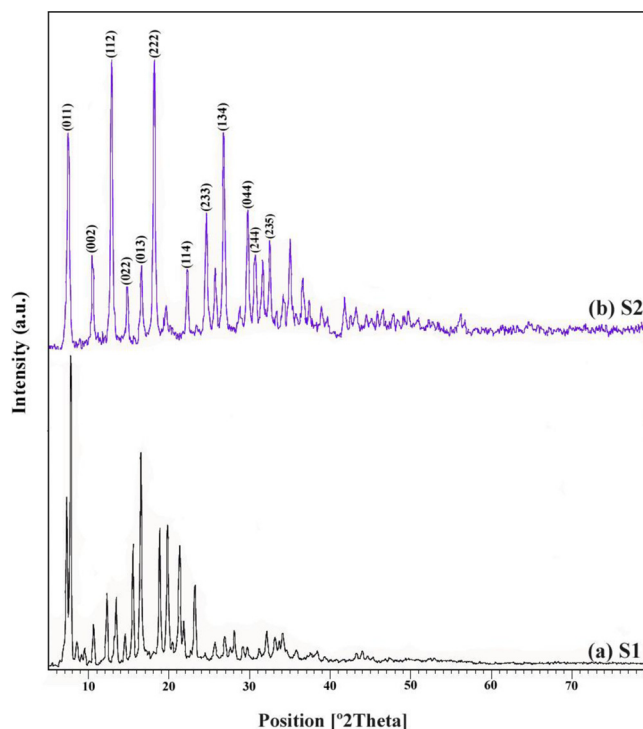


Fig. 1. PXRD patterns of (a) the as-obtained ZIF-7 lp-phase (S1) (b) of the as-synthesized ZIF-8 (S2).

2 times and then dried in the air after centrifugation.

3. Results and discussion

3.1. Framework and textural characterization

As shown in Fig. 1a, the sharp characteristics peaks at $2\theta = 7.2^\circ$ and $2\theta = 7.7^\circ$ and the other peaks in X-ray diffraction (XRD) patterns of the as-obtained sample demonstrate efficacious incorporation with the SOD-type of microporous ZIF-7 (lp-phase, S1) [50–52]. XRD patterns of ZIF-8 (S2) which is depicted in Fig. 1b also confirming the formation of SOD-type without any additional peaks indexed to (011), (002), (112), (022), (013), (222), (114), (233), (134), (044), (244) and (235) diffraction lines, respectively, which is in accordance with those reported previously [51,53,54]. Fig. 2a and b depicts the FT-IR spectra of as-obtained S1, bIM, and 2-mIM, as-produced S2, respectively. There are broad peak ranges from 2200 to 3400 cm⁻¹ with the maximum peak at the center around 2800 cm⁻¹ as well as the sharp band situated at 1408 cm⁻¹ (N–H···N stretching and bending vibrations of bIM, respectively) and sharp band at 3130 cm⁻¹ and weak band near 1823 cm⁻¹ due to C–H are ascribed to stretching and bending vibrations of 2-mIM, respectively. After full deprotonation of nitrogen atoms, all of those peaks disappear suggesting that ZIF-7 and ZIF-8 were fabricated successfully [51,55–59].

The morphology of S1 is composed of an average size of 1–2 μm cubic and smaller spherical crystals. Also, S2 particles are made up of 500 nm to 1 μm average size such that indicating both S1 and S2 have been formed from low-ordered crystals with the mean size of 500 nm to 1 μm and 200–500 nm for S1 and S2, respectively, illustrated by FE-SEM in Fig. 3a–b representing integrated micrometer-scaled cubic, spherical and to some extent rhombic-dodecahedron structures which are relatively identical to those formerly prepared [53,54].

Taking into account, the hysteresis loop suggesting the dual meso/microporous trait of ZIF-7 because of the interparticle mesopores in which nitrogen molecules are not penetrable to small windows of ZIF-7 [54–56,60,61]. Besides, due to the larger kinetic diameter of N₂

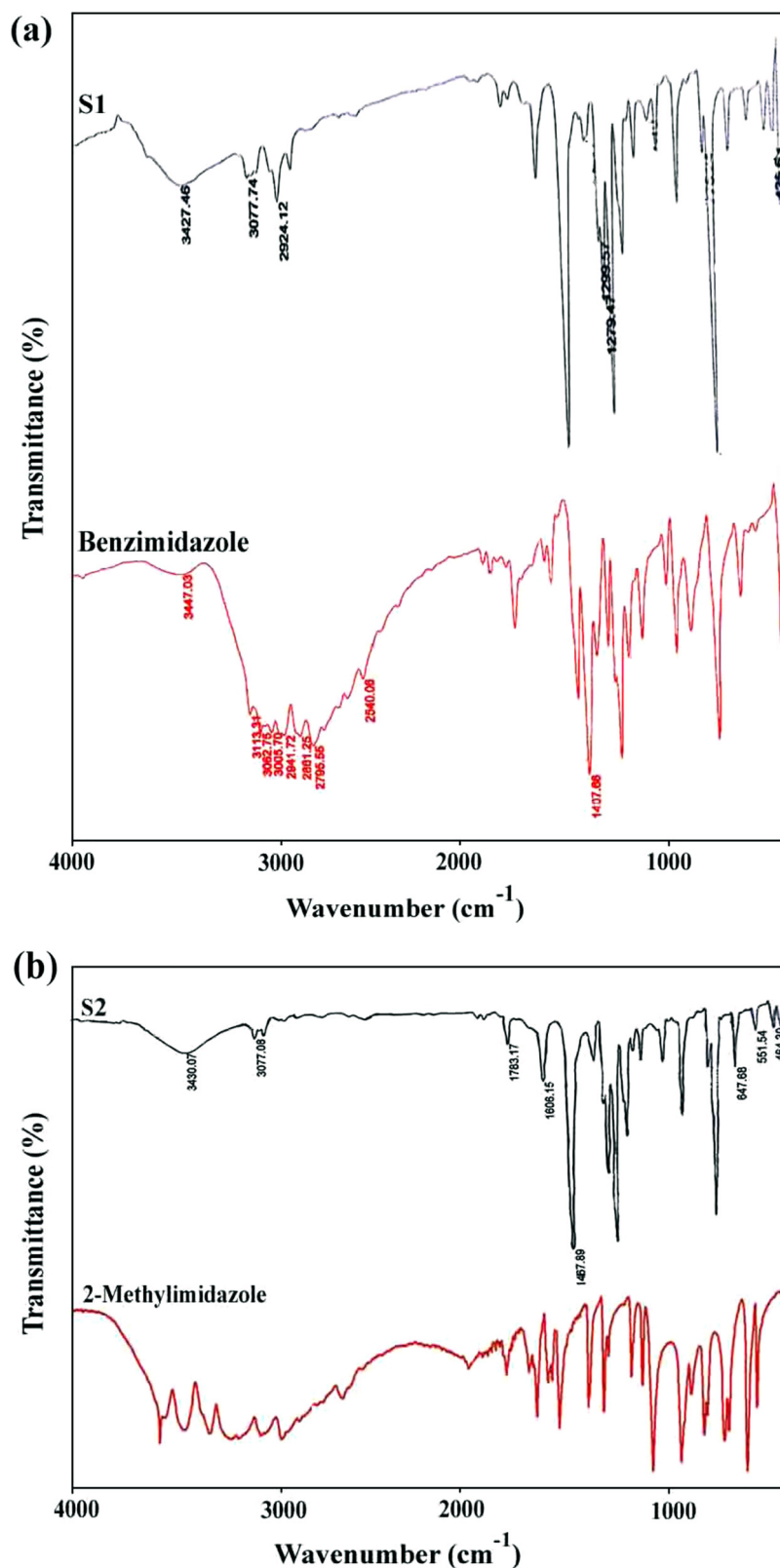


Fig. 2. FT-IR spectra of (a) BIM and S1 (b) 2-mIM and S2.

(~ 0.36 nm) than the aperture size of ZIF-7 (~ 0.3 nm) [60,63], N_2 cannot enter into ZIF-7 pores [62,63]. In comparison with relatively smaller CO_2 (kinetic diameter of 0.33 nm) than that of N_2 and considering the flexible structure of ZIF-7 [61,50,54], CO_2 molecules are much more achievable to the cavities. Type I isotherm CO_2 ads/des of

the as-prepared ZIF-7 lp-phase presents in Fig. 4a demonstrating a gate-opening phenomenon near at 20 kPa and also flexible property of the framework is indicated by the hysteresis loop. The great CO_2 adsorption capacity of about $58.32 \text{ cm}^3 \text{ g}^{-1}$ at 115 kPa represents that CO_2 is not degassed easily throughout the framework of S1 [50,52,61,64,65].

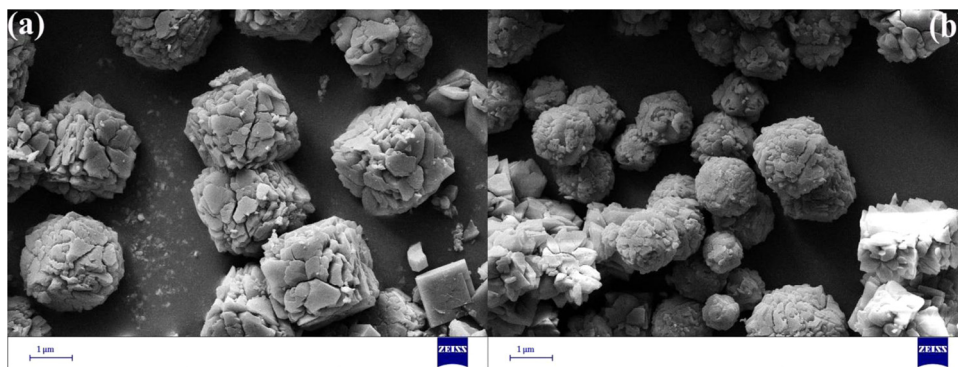


Fig. 3. FE-SEM images of (a) S1 and (b) S2.

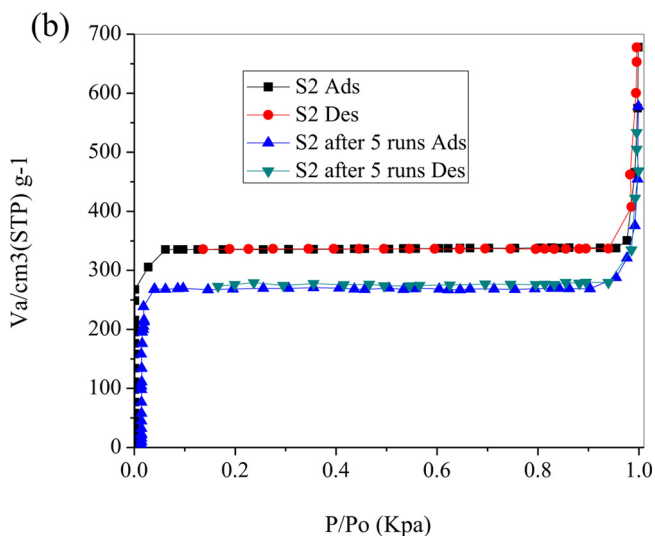
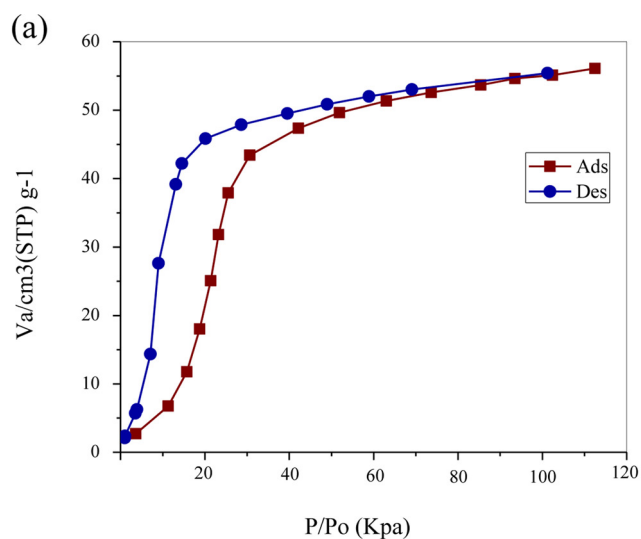


Fig. 4. (a) CO₂ ads/des isotherm of S1 at 273 K and (b) N₂ ads/des diagram of S2 (black squares and red circles) and S2 after 5 runs (blue and green triangles) at 77 K. (For interpretation of the references to colour in this figure legend, the reader is referred to the web version of this article.)

Inversely, the type I nitrogen isotherm of S2 (Fig. 4b, black squares, and red circles) displays the presence of micropores and macropores proved by high N₂ uptake at relatively low and high pressures which is made during packing of ZIF-8 crystals, respectively. Total pore volume and micropore volume of as-obtained ZIF-8 are about 1.09 and 0.60 cm³ g⁻¹, respectively. Furthermore, S_{BET} was obtained 1156 m²/g

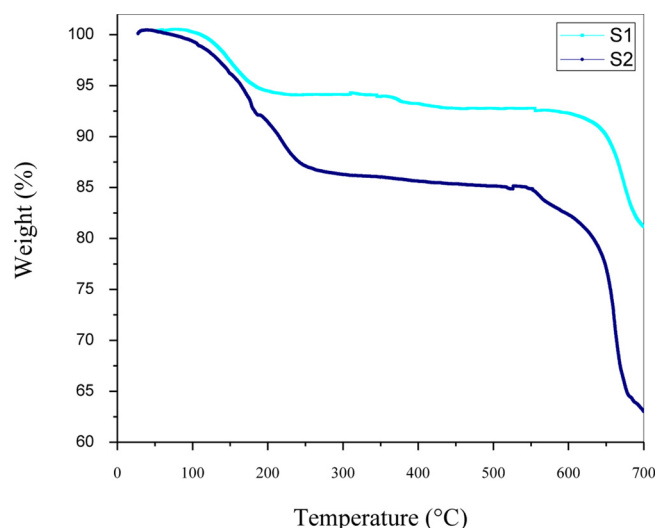


Fig. 5. TGA curves of S1 and S2.

showing its relatively high porosity and a high specific area in comparison to other counterparts synthesized in the severe situation [53,54].

As depicted in Fig. 5, first gradual weight loss of 6.72% up to 200 °C and 23% up to 250 °C which is displayed in thermogravimetry (TG) curves of S1 and S2 attributed to the removal of all guests in the cavities (especially ethanol) or the other species on the surface of the as-made ZIF-7 and ZIF-8 throughout the synthesis reaction, respectively. Second step weight loss of 14.46% and 54.58% of S1 and S2 from 200 to 700 °C and 250 to 675 °C related to the framework decomposition to ZnO, respectively [50,53,54,64–69].

3.2. Catalytic performance investigations

As above mentioned, intrigued by quite catalytic activity monitored by those metal-organic frameworks (MOFs) concerning organophosphates [9–13] and much better availability of Diazinon in our lab, the efficiency of ZIF materials were weighed by the hydrolytic dissociation of Diazinon.

The hydrolysis reaction of the Diazinon (LD50; Oral, rat 66 mg/kg) to its comparatively much less toxic compounds [70–73]; 2-isopropyl-6-methyl-4-pyrimidinol (IMP) (LD50; Oral, rat 2700 mg/kg) and *O,O*-diethyl phosphorothioic acid (PA) (LD50; Oral, rat 4510 mg/kg), the hydrolysis products, using ZIFs in aqueous buffer solution illustrates in Scheme 1. Additionally, all the toxicity degrees related to Diazinon and their hydrolysis products (PA and IMP) were provided in Table 2.

As shown in Fig. 6a and b, in situ ³¹P NMR spectra measurements demonstrating the abrupt degradation of diazinon to *O,O* diethyl

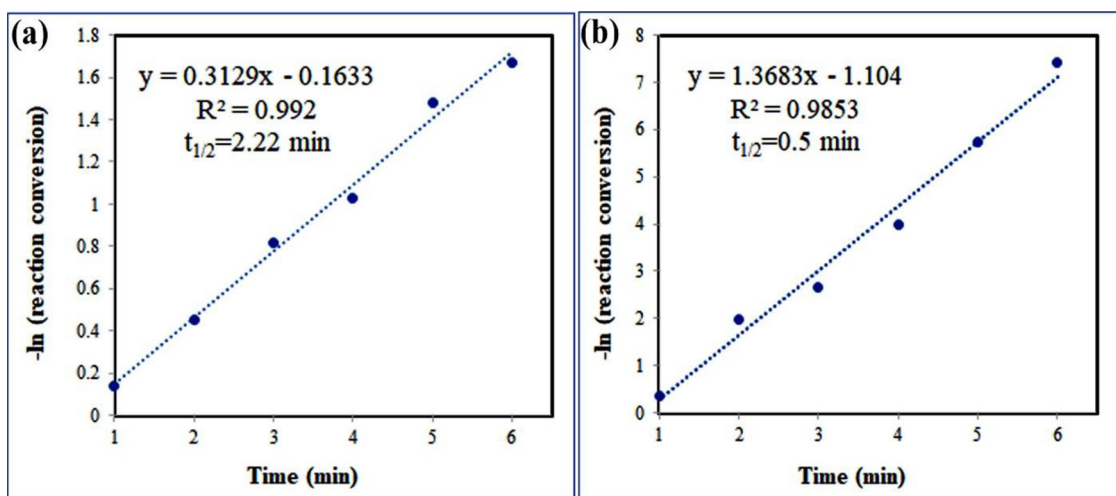


Fig. 7. Kinetic plots depicting the reaction of Diazinon with (a) S1 and (b) S2 in buffer solution, respectively. Initial half-life ($t_{1/2}$) was simply measured by drawing the obvious Ln of the conversion versus time; the slope (k) is correlated to the half-life by $t_{1/2} = \ln 2/k$.

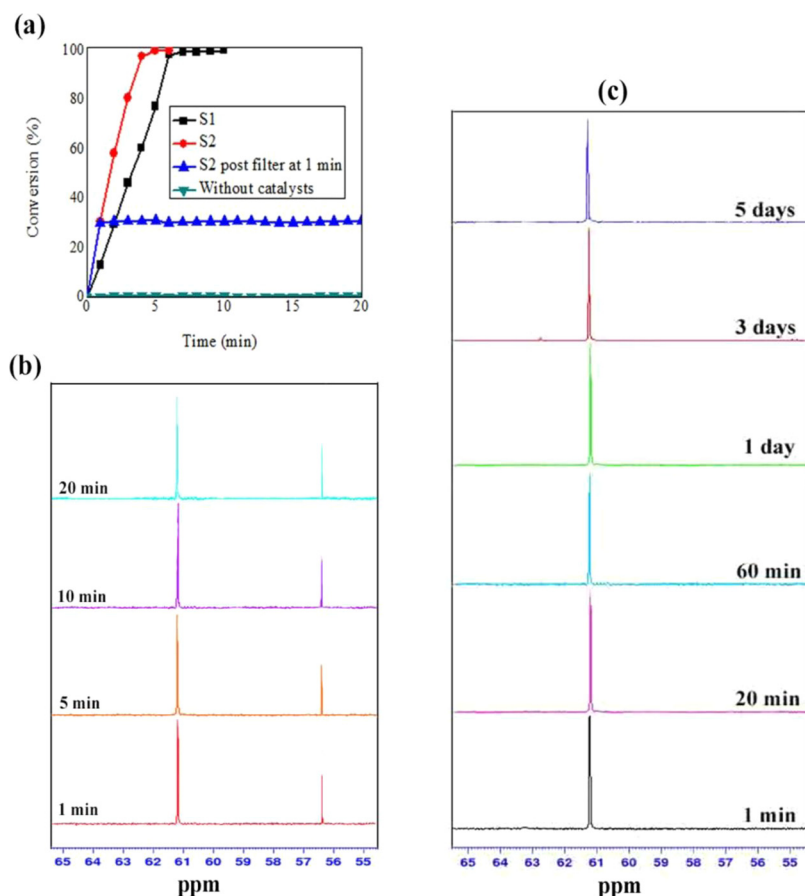


Fig. 8. (a) Reaction conversion percent/time diagram of Diazinon in the presence of S1 (black squares), S2 (red circles), post-filtration of S2 solution after 1 min (blue triangles) and in the absence of catalyst (green triangles) and ^{31}P NMR spectra of (b) S2 post-filter in the period of 1–20 min and of (c) Diazinon without catalyst in different times from 1 min to 5 days at ambient temperature, respectively. (For interpretation of the references to colour in this figure legend, the reader is referred to the web version of this article.)

the catalyst. However, the ^{31}P NMR peaks of Diazinon were collected without the catalyst in aqueous solution at 1, 20, 60 min, 1 day, 3 and 5 days (Fig. 8c). Meanwhile, the conversion after 20 min and 5 days accounted only up to less than 0.1% and 0.2% (green triangles in Fig. 8a) altogether the ^{31}P NMR of Diazinon in Fig. 8c affirming the reaction did not proceed remarkably without catalyst even over 5 days.

All of these monitoring describe clearly the complete fracture of the P–O bond in the presence of catalysts and much more comparably excellent effectiveness of S2 than that of S1 after 4 min versus 6 min as well. Given these, therefore, S2 was opted as an optimized sample for

more investigations not to perform much more excessive work to show their potential competence in cleavage of organophosphates.

Fortunately, to a great extent of precision likewise ^{31}P NMR investigations and encouraged by it, HPLC measurements that were conducted on optimized S2 is again an indication of fast completion of hydrolysis reaction by S2 over a period of 4 min. Fig. 9a presents the swift growth of IMP peak intensity at the retention time of 1.8 min versus that of Diazinon at 6.4 min, endorses the bond breakage. It explicitly would be occurred by ZIF in an exact optional attack of the P–O moiety in Diazinon which would be applicable to the other

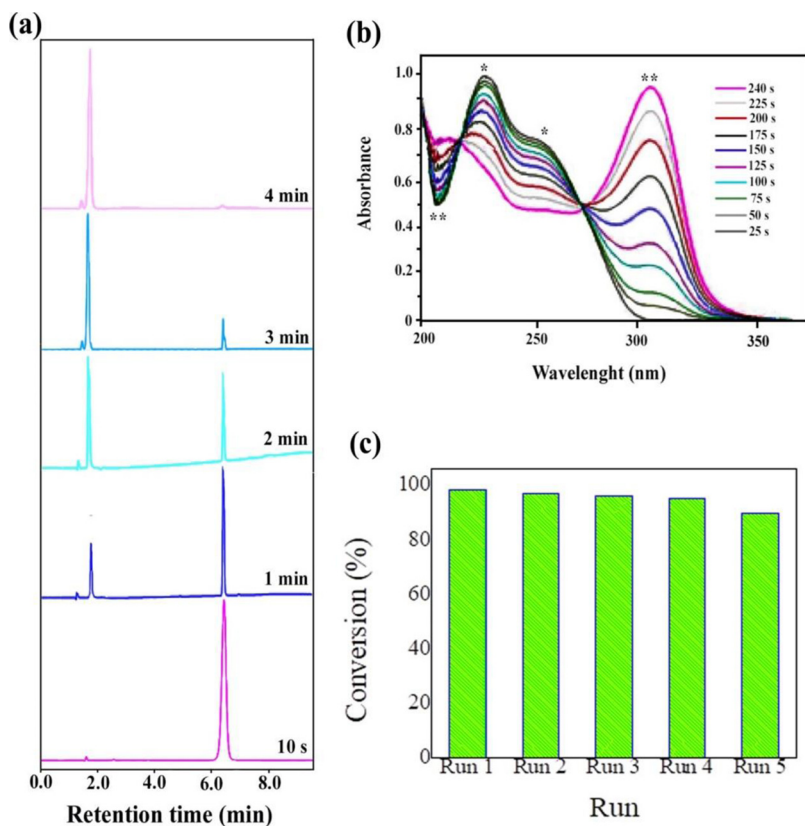


Fig. 9. Hydrolysis progress of Diazinon (6.4 min) to IMP (1.8 min) by (a) HPLC spectra and (b) UV-vis spectra (* displays the absorbance at which Diazinon observes and ** indicates the absorbance of IMP absorbs) demonstrating degradation has been happened at the times between 0–4 min using optimized S2, respectively (c) Profile of conversion percentage versus 5 successive runs.

organophosphates [75,76]. Furthermore, the conversion percentage of each time were 32.28, 61.53, 79.45 and 99.56% and also product yields were 5.82, 11.08, 14.3 and 17.93 μmol according to the initial input reactant (Diazinon; 18 μmol) for 1, 2, 3 and 4 min after addition of Diazinon, respectively. The comparatively similar results earned by HPLC data also indicating the great harmony with the spectra monitored by ^{31}P NMR instrument (Fig. 6b).

Fig. 9b represents the UV/Vis spectra of the hydrolysis reaction in the presence of the optimized S2 with the interval time of each 25 s up to 4 min where the one asterisk mark (*) in the range of 225–255 nm and two asterisks ones (**) spanning over about 200–220 and 300–350 nm are ascribed to Diazinon and IMP, respectively. These wavelengths at which simultaneously the absorbance of reagent (Diazinon) are descending and those of product (IMP) are ascending; thereby explaining the particularly selective dissociation of P–O bond in Organophosphates by ZIF and subsequently illustrating that these data are in line again with the identical afore-reported contributions [9,10,77].

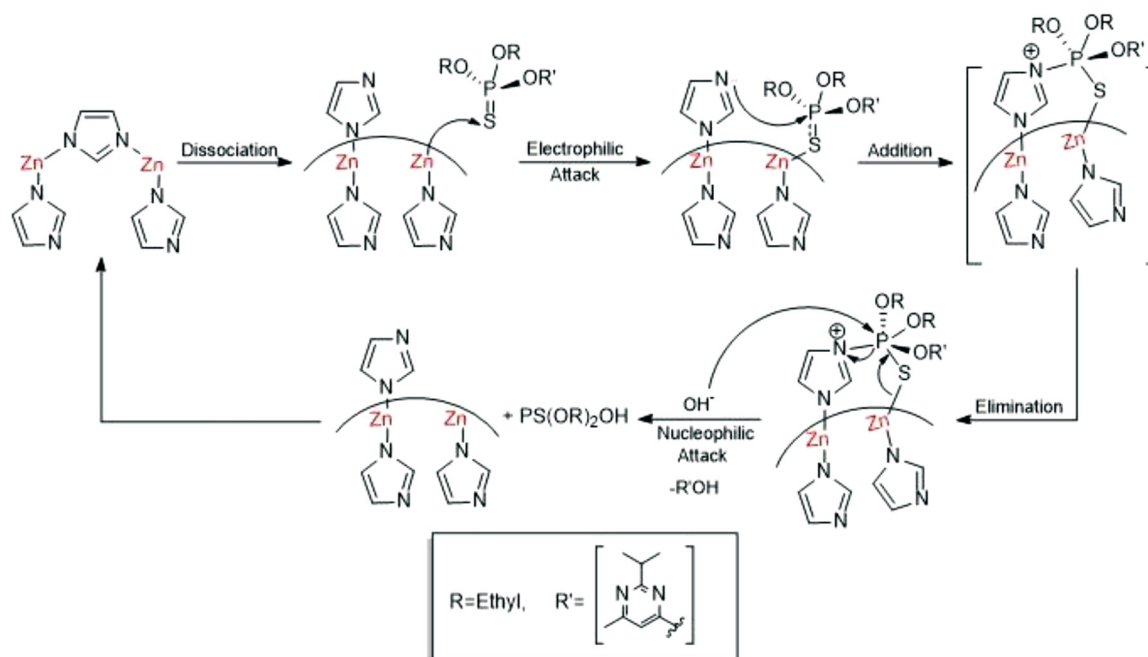
3.3. Hydrolysis reaction mechanism

Actually, the whole process would be comprehended better in a meaningfully visual depiction by its suggested mechanism which is hypothetically proposed as a main overall procedure for catalytic degradation of OPs. As can be seen in Scheme 2, the process commences with the first step which the imidazolate ligands on the surface of the catalyst may detach partly instantly duo to the differences of charges happened by solvent and the other components throughout the reaction. Next, after the dissociation of linker, an electrophilic attack would be taken placed by Zn (II) Lewis acid center to the sulfur atom of the P=S bond of Diazinon to construct a complex resulting in making P=S bond more polarized and triggered it to being more prone to activate the acceleration of the nucleophilic attack performed by free non-bonding nitrogen atom on another Zn atom in the further step.

Subsequently, free pair electrons of nitrogen which serves as Lewis base would efficaciously enhance the reaction directly by attachment attack to the sufficiently high polarized P atom of the P=S bond and then reaches a highly energetic transition state (TS; shown in bracket). Further, R'OH moiety (IMP; observed by UV-vis-equipped HPLC accompanied by UV-vis spectroscopy), simultaneously is eliminated by the second nucleophilic attack of OH^- ions generated from H_2O solvent molecules (*N*-ethylmorpholine; buffer solution function as wiping out agent of acidic byproduct (here including R'OH) and deprotonating agent of water as well as to elevate the speed of the reaction [78,79]) again to phosphorus atom to terminate the reaction by forming the other moiety $\text{PS}(\text{OR})_2\text{OH}$ (PA; monitored by ^{31}P NMR). In this stage the process begins itself again by reverting of the catalyst to its initial form. In our case, the synergistic catalytic activation of the OP imposed by concomitantly Lewis acid-cum-Lewis base behavior of ZIF would be practically beheld graphically here to boost the detoxification of such deleterious compound [14,80–84].

3.4. Recycling and inviolability inspections

Fascinatedly enough, the surface areas of S2 diminished from 1156 to 846 m^2/g after 5 sequential reactions which have been depicted in Fig. 4b (blue and green triangles) stating that the conversion percentages were lessened from 98.35 in run 1 to 97.04 (run 2), 96.01 (run 3), 95.06 (run 4), and to 90.04% in run 5 is the delineation of the re-utilization of S2 would be done after consecutive cycles with little decrease in its efficiency (Fig. 9c). With having this said, the assumption is also reinforced by the color alternation of S2 from white to pale yellow. As a consequence, ZIF retained its stability during process which was confirmed by excellent durability of optimized S2 architecture and was checked by X-ray diffraction (XRD), FT-IR spectra and FE-SEM images depicted in Figs. 10, 11 and 12, respectively. Within the hydrolysis process though the catalytic efficiency was not declined through the blocking of the S2 windows and voids by diverse species in solution; in



Scheme 2. Proposed overall hypothetical catalytic detoxification mechanism.

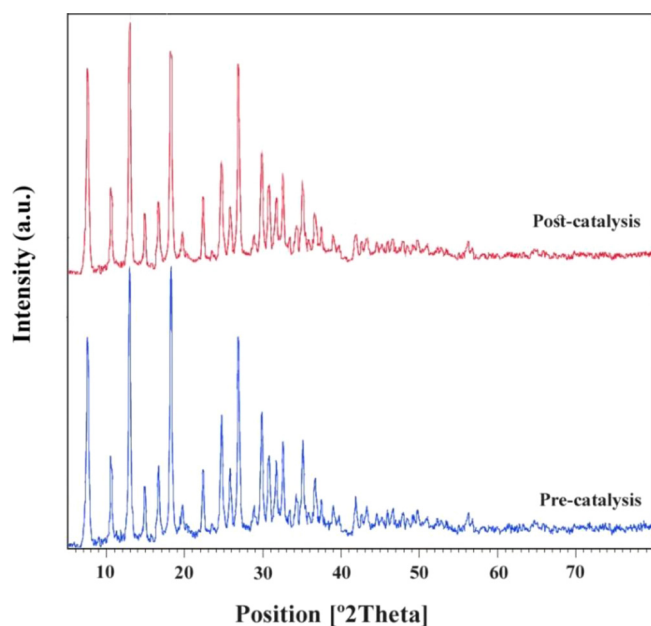


Fig. 10. PXRD patterns of pre- and post-catalysis of optimized S2 after 5 sequential cycles.

turn, representing that the catalyst maintains its post-catalysis crystal structure inviolability after 5 incessant cycles. As can be observed, the comparison of the pre- and post-catalysis patterns, spectra and images vividly presents its approximately wonderful unspoiled framework exposure to the simulant and solvent in the solution. Not having envisaged previously that the pore closure has no considerably high impact on hydrolysis enhancement alongside even much more larger size of Diazinon than the aperture size of ZIF (~ 0.3 nm) [50,61–64], As a result, it causes not to pass through the gate of ZIF to locate into the innermost of ZIF structure; successively regarding that reaction would take place uniquely on the outer sites of ZIF framework. Thereby, it can be deduced that the reaction is happening extremely swift.

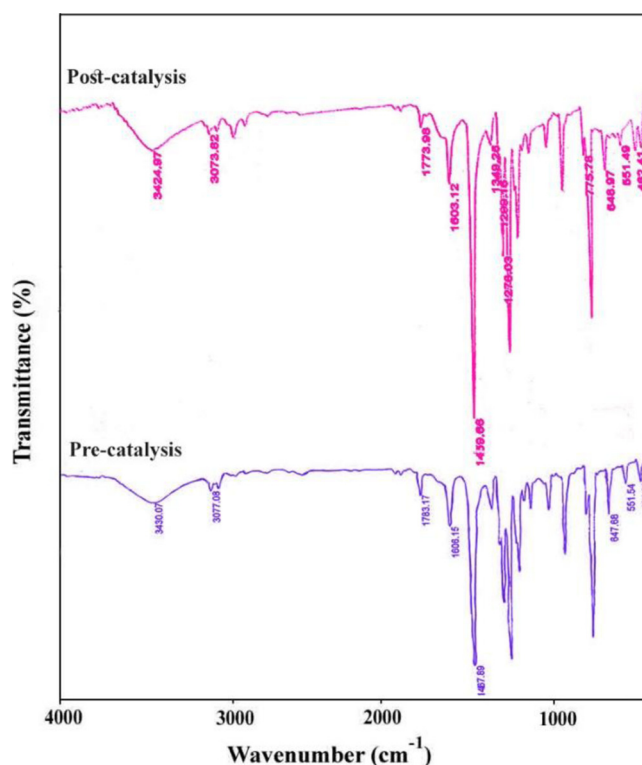


Fig. 11. FT-IR spectra of pre- and post-catalysis of optimized S2 after 5 incessant successions.

4. Conclusions and outlooks

By and large, Successfully, we here have proved for the first time the hydrolysis degradation of OP pesticide (Diazinon) was performed by a series of ZIFs in aqueous solution demonstrating high capability of these materials in catalytic detoxification of organophosphates simulant in comparison to those have been studied ever which have proven their catalytic efficiency too time-consuming. Unequivocally, such swift catalytic detoxification of the organophosphate (Diazinon) was

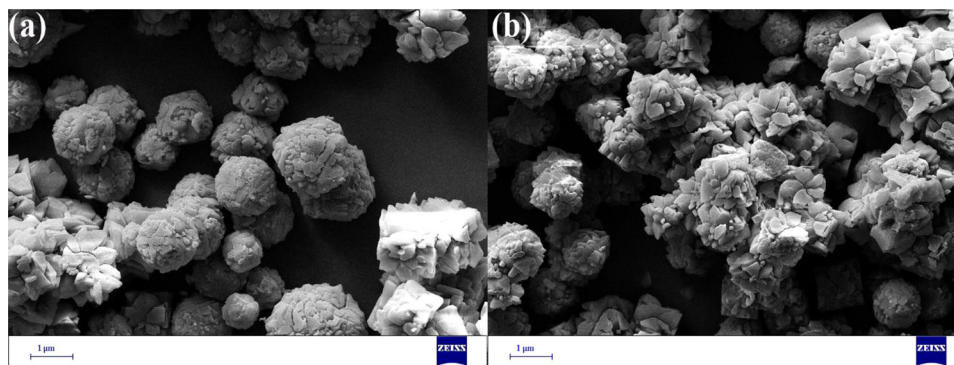


Fig. 12. FE-SEM images of (a) pre- and (b) post-catalysis of optimized S2 and after 5 consecutive runs, respectively.

confirmed by ^{31}P NMR and HPLC within 4 min, favorably. As a consequence, all the observations illustrated here also approve that ZIFs materials, particularly wondrous optimized S2 (ZIF-8), have been prominent for their chemical and thermal stabilities in harsh media definitely acknowledging its marvelous perseverance and relatively high performance after several incessant catalysis reactions which can be led that the usage of them would be as an exceptional competitor and premium alternative material to those MOFs investigated, so far.

CRedit authorship contribution statement

Arash Ebrahimi: Conceptualization, Investigation, Writing - original draft. **Ehsan Nassireslami:** Supervision, Writing - review & editing, Project administration. **Ramin Zibaseresht:** Supervision, Methodology, Resources. **Maedeh Mohammadsalehi:** Software, Formal analysis, Data curation.

Declaration of Competing Interest

The authors declare that they have no known competing financial interests or personal relationships that could have appeared to influence the work reported in this paper.

Acknowledgments

Honorably, we should express our supreme gratitude for the financial support of this work from Aja University of Medical Sciences.

References

- [1] K. Kim, O.G. Tsay, D.A. Atwood, D.G. Churchill, *Chem. Rev.* 111 (2011) 5345–5403, <https://doi.org/10.1021/cr100193y>.
- [2] M.R. Sambrook, S. Notman, *Chem. Soc. Rev.* 42 (2013) 9251–9267, <https://doi.org/10.1039/C3CS60230C>.
- [3] D.B. Barr, R. Allen, A.O. Olsson, R. Bravo, L.M. Caltabiano, A. Montesano, J. Nguyen, S. Udunka, D. Walden, R.D. Walker, G. Weerasekera, R.D. Whitehead Jr., S.E. Schober, L.L. Needham, *Environ. Res.* 99 (2005) 314–326, <https://doi.org/10.1016/j.envres.2005.03.012>.
- [4] S.M. Ross, I.C. McManus, V. Harrison, O. Mason, *Crit. Rev. Toxicol.* 43 (2013) 21–44, <https://doi.org/10.3109/10408444.2012.738645>.
- [5] J.R. Roberts, C.J. Karr, *Pediatrics* 130 (2012) 1765–1788, <https://doi.org/10.3109/1040844403.0>.
- [6] J.L. Acero, F.J. Benítez, F.J. Real, M. González, *J. Hazard. Mater.* 153 (2008) 320–328, <https://doi.org/10.1016/j.jhazmat.2007.08.051>.
- [7] A. Chanda, S.K. Khetan, D. Banerjee, A. Ghosh, T.J. Collins, *J. Am. Chem. Soc.* 128 (2006) 12058–12059, <https://doi.org/10.1021/ja064017e>.
- [8] B.M. Smith, *Chem. Soc. Rev.* 37 (2008) 470–478, <https://doi.org/10.1039/b705025a>.
- [9] M.J. Katz, J.E. Mondloch, R.K. Totten, J.K. Park, S.T. Nguyen, O.K. Farha, J.T. Hupp, *Angew. Chem. Int. Ed.* 53 (2014) 497–501, <https://doi.org/10.1002/ange.201307520>.
- [10] S.-Y. Moon, Y. Liu, J.T. Hupp, O.K. Farha, *Angew. Chem. Int. Ed.* 54 (2015) 6795–6799, <https://doi.org/10.1002/anie.201502155>.
- [11] Z. Chen, T. Islamoglu, O.K. Farha, *ACS Appl. Nano Mater.* 2 (2019) 1005–1008, <https://doi.org/10.1021/acsnano.8b02292>.
- [12] P. Li, S.-Y. Moon, M.A. Guelta, L. Lin, D.A. Gomez-Gualdrón, R.Q. Snurr, S.P. Harvey, J.T. Hupp, O.K. Farha, *ACS Nano* 10 (2016) 9174–9182, <https://doi.org/10.1021/acsnano.6b04996>.
- [13] S.-Y. Moon, G.W. Wagner, J.E. Mondloch, G.W. Peterson, J.B. DeCoste, J.T. Hupp, O.K. Farha, *Inorg. Chem.* 54 (2015) 10829–10833, <https://doi.org/10.1021/acs.inorgchem.5b01813>.
- [14] A.M. Plonka, Q. Wang, W.O. Gordon, A. Balboa, D. Troya, W. Guo, C.H. Sharp, S.D. Senanayake, J.R. Morris, C.L. Hill, A.I. Frenkel, *J. Am. Chem. Soc.* 139 (2017) 599–602, <https://doi.org/10.1021/jacs.6b11373>.
- [15] J. Zhao, D.T. Lee, R.W. Yaga, M.G. Hall, H.F. Barton, I.R. Woodward, C.J. Oldham, H.J. Walls, G.W. Peterson, G.N. Parsons, *Angew. Chem.* 128 (2016) 1–6, <https://doi.org/10.1002/anie.201606656>.
- [16] E. Lopez-Maya, C. Montoro, L.M. Rodríguez-Albelo, S.D.A. Cervantes, A.A. Lozano-Prez, J.L. Cens, J.A.R. Navarro, *Angew. Chem. Int. Ed.* 54 (2015) 6790–6794, <https://doi.org/10.1002/anie.201502094>.
- [17] C. Montoro, F. Linares, E.Q. Procopio, I. Senkova, S. Kaskel, S. Galli, N. Masciocchi, E. Barea, J.A.R. Navarro, *J. Am. Chem. Soc.* 133 (2011) 11888–11891, <https://doi.org/10.1021/ja2042113>.
- [18] A. Roy, A.K. Srivastava, B. Singh, T.H. Mahato, D. Shah, A.K. Halve, *Microporous Mesoporous Mater.* 162 (2012) 207–212, <https://doi.org/10.1016/j.micromeso.2012.06.011>.
- [19] G.W. Peterson, G.W. Wagner, *J. Porous Mater.* 21 (2014) 121–126, <https://doi.org/10.1007/s10934-013-9755-6>.
- [20] S.-Y. Moon, G.W. Wagner, J.E. Mondloch, G.W. Peterson, J.B. DeCoste, J.T. Hupp, O.K. Farha, *Inorg. Chem.* 54 (2015) 10829–10833, <https://doi.org/10.1021/acs.inorgchem.5b01813>.
- [21] P. Nunes, A.C. Gomes, M. Pillinger, I.S. Gonçalves, M. Abrantes, M. Abrantes, *Microporous Mesoporous Mater.* 208 (2015) 21–29, <https://doi.org/10.1016/j.micromeso.2015.01.016>.
- [22] W. Chaikittisilp, N.L. Torad, C. Li, M. Imura, N. Suzuki, S. Ishihara, K. Ariga, Y. Yamauchi, *Chem. Eur. J.* 20 (2014) 4217–4221, <https://doi.org/10.1002/chem.201304404>.
- [23] A.M. Rashidi, M. Mirzaei, S. Khodabakhshi, *J. Nat. Gas Sci. Eng.* 25 (2015) 103–109, <https://doi.org/10.1016/j.jngse.2015.04.037>.
- [24] J. Tang, Y. Yamauchi, *Nat. Chem.* 8 (2016) 638–639, <https://doi.org/10.1038/nchem.2548>.
- [25] R.R. Salunkhe, C. Young, J. Tang, T. Takei, Y. Ide, N. Kobayashi, Y. Yamauchi, *Chem. Commun.* 52 (2016) 4764–4767, <https://doi.org/10.1039/C6CC00413J>.
- [26] W. Zhang, X. Jiang, Y. Zhao, A. Carné-Sánchez, V. Malgras, J. Kim, J.H. Kim, S. Wang, J. Liu, J.-S. Jiang, Y. Yamauchi, M. Hu, *Chem. Sci.* 8 (2017) 3538–3546, <https://doi.org/10.1039/C6SC04903F>.
- [27] E. Fernandez-Bartolome, J. Santos, S. Khodabakhshi, L.J. McCormick, S.J. Teat, C.S. de Pipaon, J.R. Galan-Mascarós, N. Martín, J.S. Costa, *Chem. Commun.* 54 (2018) 5526–5529, <https://doi.org/10.1039/C8CC01561A>.
- [28] K. Sumida, D.L. Rogow, J.A. Mason, T.M. McDonald, E.D. Bloch, Z.R. Herm, T.-H. Bae, J.R. Long, *Chem. Rev.* 112 (2012) 724–781, <https://doi.org/10.1021/cr2003272>.
- [29] J.V.D. Bergh, C. Gücüyener, E.A. Pidko, E.J.M. Hensen, J. Gascon, F. Kaptejin, *Chem. Eur. J.* 17 (2011) 8832–8840, <https://doi.org/10.1002/chem.201100958>.
- [30] T. Li, Y. Pan, K.-V. Peinemann, Z. Lai, *J. Membr. Sci.* 425–426 (2013) 235–242, <https://doi.org/10.1016/j.memsci.2012.09.006>.
- [31] T. Rodenas, M. van Dalen, E. Garcia-Prez, P. Serra-Crespo, B. Zornoza, F. Kaptejin, J. Gascon, *Adv. Funct. Mater.* 24 (2014) 249–256, <https://doi.org/10.1002/adfm.201203462>.
- [32] Y. Cui, Y. Yue, G. Qian, B. Chen, *Chem. Rev.* 112 (2011) 1126–1162, <https://doi.org/10.1021/cr200101d>.
- [33] J. Liu, L. Chen, H. Cui, J. Zhang, L. Zhang, C.-Y. Su, *Chem. Soc. Rev.* 43 (2014) 6011–6061, <https://doi.org/10.1039/C4CS00094C>.
- [34] T. Zhang, W. Lin, *Chem. Soc. Rev.* 43 (2014) 5982–5993, <https://doi.org/10.1039/C4CS00103F>.
- [35] Z. Hu, B.J. Deibert, J. Li, *Chem. Soc. Rev.* 43 (2014) 5815–5840, <https://doi.org/10.1039/C4CS00010B>.
- [36] L.E. Kreno, K. Leong, O.K. Farha, M. Allendorf, R.P.V. Duyne, J.T. Hupp, *Chem. Rev.* 112 (2011) 1105–1125, <https://doi.org/10.1021/cr200324t>.
- [37] P. Horcajada, T. Chalati, C. Serre, B. Gillet, C. Sebrie, T. Baati, J.F. Eubank, D. Heurtaux, P. Clayette, C. Kreuz, J.-S. Chang, Y.K. Hwang, V. Marsaud, P.-

- N. Bories, L. Cynober, S. Gil, G. Frey, P. Couvreur, R. Gref, *Nat. Mater.* 9 (2010) 172–178, <https://doi.org/10.1038/nmat2608>.
- [38] M. Saito, T. Toyao, K. Ueda, T. Kamegawa, Y. Horiuchi, M. Matsuoka, *Dalton Trans.* 42 (2013) 9444–9447, <https://doi.org/10.1039/C3DT50593F>.
- [39] J.C. Tan, T.D. Bennett, A.K. Cheetham, *Proc. Natl. Acad. Sci. U. S. A.* 107 (2010) 9938–9943, <https://doi.org/10.1073/pnas.1003205107>.
- [40] B. Chen, Z. Yang, Y. Zhu, Y. Xia, J. Mater. Chem. A. 2 (2014) 16811–16831, <https://doi.org/10.1039/C4TA02984D>.
- [41] M.Q. Zhu, D. Srinivas, S. Bhogeswararao, P. Ratnasamy, M.A. Carreon, *Catal. Commun.* 32 (2013) 36–40, <https://doi.org/10.1016/j.catcom.2012.12.003>.
- [42] C. Chizallet, S. Lazare, D. Bazer-Bachi, F. Bonnier, V. Lecocq, E. Soyer, A.A. Quoineaud, N. Bats, *J. Am. Chem. Soc.* 132 (2010) 12365–12377, <https://doi.org/10.1021/ja103365s>.
- [43] A.N. Bigley, F.M. Raushel, *Biochim. Biophys. Acta* 1834 (2013) 443–453, <https://doi.org/10.1016/j.bbapap.2012.04.004>.
- [44] K.-Y. Wong, J. Gao, *Biochemistry* 46 (2007) 13352–13369, <https://doi.org/10.1021/bi700460c>.
- [45] M.J. Katz, S.-Y. Moon, J.E. Mondloch, M.H. Beyzavi, C.J. Stephenson, J.T. Hupp, O.K. Farha, *Chem. Sci.* 6 (2015) 2286–2291, <https://doi.org/10.1039/C4SC03613A>.
- [46] S.G. Ryu, M.-K. Kim, M. Park, S.O. Jang, S.H. Kim, H. Jung, *Microporous Mesoporous Mater.* 274 (2019) 9–16, <https://doi.org/10.1016/j.micromeso.2018.07.027>.
- [47] R. Gil-San-Millan, E. López-Maya, M. Hall, N.M. Padial, G.W. Peterson, J.B. DeCoste, L.M. Rodríguez-Albelo, J.E. Oltra, E. Barea, J.A.R. Navarro, *ACS Appl. Mater. Interfaces* 9 (2017) 23967–23973, <https://doi.org/10.1021/acsami.7b06341>.
- [48] M.C. de Koning, M.V. Grol, T. Breijer, *Inorg. Chem.* 56 (2017) 11804–11809, <https://doi.org/10.1021/acs.inorgchem.7b01809>.
- [49] Z. Chen, T. Islamoglu, O.K. Farha, *ACS Appl. Nano Mater.* 2 (2019) 1005–1008, <https://doi.org/10.1021/acsanm.8b02292>.
- [50] A. Ebrahimi, M.R. Mansournia, *Chem. Phys.* 511 (2018) 33–45, <https://doi.org/10.1016/j.chemphys.2018.06.003>.
- [51] K.S. Park, Z. Ni, A.P. Côté, J.Y. Choi, R. Huang, F.J. Uribe-Romo, H.K. Chae, M. O'Keefe, O.M. Yaghi, *Proc. Natl. Acad. Sci. U.S.A.* 103 (2006) 10186–10191, <https://doi.org/10.1073/pnas.0602439103>.
- [52] Y.S. Li, H. Bux, A. Feldhoff, G.L. Li, W.S. Yang, J. Caro, *Adv. Mater.* 22 (2010) 3322–3326, <https://doi.org/10.1002/adma.201000857>.
- [53] M. He, Jianfeng Yao, Q. Liu, K. Wang, F. Chen, H. Wang, *Microporous Mesoporous Mater.* 184 (2014) 55–60, <https://doi.org/10.1016/j.micromeso.2013.10.003>.
- [54] J. Qian, F. Sun, L. Qin, *Mater. Lett.* 82 (2012) 220–223, <https://doi.org/10.1016/j.matlet.2012.05.077>.
- [55] Y. Pan, Y. Liu, G. Zeng, L. Zhao, Z. Lai, *Chem. Commun.* 47 (2011) 2071–2073, <https://doi.org/10.1039/C0CC05002D>.
- [56] Y. Hu, H. Kazemian, S. Rohani, Y.N. Huang, Y. Song, *Chem. Commun.* 47 (2011) 12694–12696, <https://doi.org/10.1039/C1CC15525C>.
- [57] T. Li, Y. Pan, K.-V. Peinemann, Z. Lai, *J. Membr. Sci.* 425 (2013) 235–242, <https://doi.org/10.1016/j.memsci.2012.09.006>.
- [58] T. Yang, Y. Xiao, T.-S. Chung, *Energy Environ. Sci.* 4 (2011) 4171–4180, <https://doi.org/10.1039/C1EE01324F>.
- [59] J. Cravillon, S. Munzer, S.J. Lohmeier, A. Feldhoff, K. Huber, M. Wiebecke, *Chem. Mater.* 21 (2009) 1410–1412, <https://doi.org/10.1021/cm900166h>.
- [60] M. He, J. Yao, Q. Liu, Z. Zhong, H. Wang, *Dalton Trans.* 42 (2013) 16608–16613, <https://doi.org/10.1039/C3DT52103F>.
- [61] M. He, J. Yao, L. Li, K. Wang, F. Chen, H. Wang, *ChemPlusChem* 78 (2013) 1222–1225, <https://doi.org/10.1002/cplu.201300193>.
- [62] S. Horike, S. Shimomura, S. Kitagawa, *Nat. Chem.* 1 (2009) 695–704, <https://doi.org/10.1038/nchem.444>.
- [63] J.-R. Li, R.J. Kuppler, H.-C. Zhou, *Chem. Soc. Rev.* 38 (2009) 1477–1504, <https://doi.org/10.1039/B802426J>.
- [64] X. Wua, M.N. Shahrak, B. Yuan, S. Deng, *Microporous Mesoporous Mater.* 190 (2014) 189–196, <https://doi.org/10.1016/j.micromeso.2014.02.016>.
- [65] X. Wang, P. Huang, P. Yu, L. Yang, L. Mao, *ChemPlusChem* 79 (2014) 907–913, <https://doi.org/10.1002/cplu.201402052>.
- [66] P. Zhao, G.I. Lampronti, G.O. Lloyd, M.T. Wharmby, S. Facq, A.K. Cheetham, S.A.T. Redfern, *Chem. Mater.* 26 (2014) 1767–1769, <https://doi.org/10.1021/cm500407f>.
- [67] W. Sun, X. Zhai, L. Zhao, *Chem. Eng. J.* 289 (2016) 59–64, <https://doi.org/10.1016/j.cej.2015.12.076>.
- [68] F.-K. Shieh, S.-C. Wang, S.-Y. Leo, K.C.W. Wu, *Chem. Eur. J.* 19 (2013) 11139–11142, <https://doi.org/10.1002/chem.201301560>.
- [69] A. Ebrahimi, M.R. Mansournia, *J. Phys. Chem. Solids* 111 (2017) 12–17, <https://doi.org/10.1016/j.jpcs.2017.07.006>.
- [70] H.M. Gomma, I.H. Suffet, S.D. Faust, *Residue Reviews Vol. 29 Springer, New York*, 1969.
- [71] J. Marhold, *Avicenum Vol. 1-2 (1986) Czech Republic*.
- [72] W. Muecke, K.O. Alt, H.E. Esser, *J. Agric. Food Chem.* 18 (1970) 208–212, <https://doi.org/10.1021/jf60168a020>.
- [73] V. Aggarwal, X. Deng, A. Tuli, K.S. Goh, *Rev. Environ. Contam. Toxicol.* 223 (2013) 107–140, https://doi.org/10.1007/978-1-4614-5577-6_5.
- [74] M. Armaghan, M.M. Amini, *Arab. J. Chem.* 10 (2017) 91–99, <https://doi.org/10.1016/j.arabjc.2014.01.002>.
- [75] A.W. Abu-Qare, M.B. Abou-Donia, *J. Chromatogr. Sci.* 39 (2001) 200–204, <https://doi.org/10.1093/chromsci/39.5.200>.
- [76] M.R. Rezk, A. El-Aziz, B. El-Aleem, S.M. Khalile, O.K. El-Naggar, *J. AOAC Int.* 101 (2018) 1191–1197, <https://doi.org/10.5740/jaoacint.17-0187>.
- [77] H. Shemer, K.G. Linden, *J. Hazard. Mater.* 136 (2006) 553–559, <https://doi.org/10.1016/j.jhazmat.2005.12.028>.
- [78] S.-Y. Moon, E. Prousaloglou, G.W. Peterson, J.B. DeCoste, M.G. Hall, A.J. Howarth, J.T. Hupp, O.K. Farha, *Chem. Eur. J.* 22 (2016) 14864–14868, <https://doi.org/10.1002/chem.201603976>.
- [79] J.B. DeCoste, G.W. Peterson, *Chem. Rev.* 114 (2014) 5695–5727, <https://doi.org/10.1021/cr4006473>.
- [80] S. Lundgren, E. Wingstrand, M. Penhoat, C. Moberg, *J. Am. Chem. Soc.* 127 (2005) 11592–11593, <https://doi.org/10.1021/ja052804q>.
- [81] E. Wingstrand, S. Lundgren, M. Penhoat, C. Moberg, *Pure Appl. Chem.* 78 (2006) 409–414, <https://doi.org/10.1351/pac200678020409>.
- [82] S. Wang, L. Bromberg, H. Schreuder-Gibson, T.A. Hatton, *ACS Appl. Mater. Interfaces* 5 (2013) 1269–1278, <https://doi.org/10.1021/am302359b>.
- [83] J.M. Palomba, C.V. Credille, M. Kalaj, J.B. DeCoste, G.W. Peterson, T.M. Tovar, S.M. Cohen, *Chem. Commun.* 54 (2018) 5768–5771, <https://doi.org/10.1039/C8CC03255F>.
- [84] H. Wang, J.J. Mahle, T.M. Tovar, G.W. Peterson, M.G. Hall, J.B. DeCoste, J.H. Buchanan, C.J. Karwacki, *ACS Appl. Mater. Interfaces* 11 (2019) 21109–21116, <https://doi.org/10.1021/acsami.9b04927>.